arXiv:2006.09308v1 [eess.IV] 16 Jun 2020

Lung Segmentation and Nodule Detection in Computed Tomography Scan using a Convolutional Neural Network Trained Adversarially using Turing Test Loss

Rakshith Sathish[1], Rachana Sathish[1], Ramanathan Sethuraman[2] and Debdoot Sheet[1]

***Abstract*— Lung cancer is the most common form of cancer found worldwide with a high mortality rate. Early detection of pulmonary nodules by screening with a low-dose computed tomography (CT) scan is crucial for its effective clinical management. Nodules which are symptomatic of malignancy occupy about 0.0125 - 0.025% of volume in a CT scan of a patient. Manual screening of all slices is a tedious task and presents a high risk of human errors. To tackle this problem we propose a computationally efficient two stage framework. In the first stage, a convolutional neural network (CNN) trained adversarially using Turing test loss segments the lung region. In the second stage, patches sampled from the segmented region are then classified to detect the presence of nodules. The proposed method is experimentally validated on the LUNA16 challenge dataset with a dice coefficient of 0.984 ± 0.0007 for 10-fold cross-validation.**

I. Introduction

Lung cancer is the most common form of cancer worldwide, accounting for about 2.1 million new cases and 1.8 million deaths annually [1]. Presence of nodules is considered to be one of the precursors for lung cancer. Pulmonary nodules are radiographically opaque and measure up to 30 millimeter in diameter. Low-dose CT based imaging is performed to detect the presence of nodules [2]. The chances of survival increases significantly when diagnosed at an early stage of the cancer, thus rendering the task of nodule detection a critical one.

Manual screening of nodules in CT scans is a time consuming and stressful task which requires the expertise of an experienced radiologist. A standard CT volume has 200-400 slices while the nodules are present in only 3-5 slices. Radiologists have to manually screen the slices, identify the suspicious slices and later detect nodules. Manual screening is often plagued with false negative classifications, due to the very small size of nodules. Automation of this task can lessen the workload of manual screening and also reduce false negatives and improve cancer management outcomes through early diagnosis.

Challenges: One of the major challenges associated with the detection of lung nodules is the wide variation in appearance and spatial distribution. Nodules can be present either completely isolated within the lung parenchyma or attached to the lung walls. Characteristics of a nodule, such as texture, shape, opacity, size, etc have high variance which makes its detection a complex task.

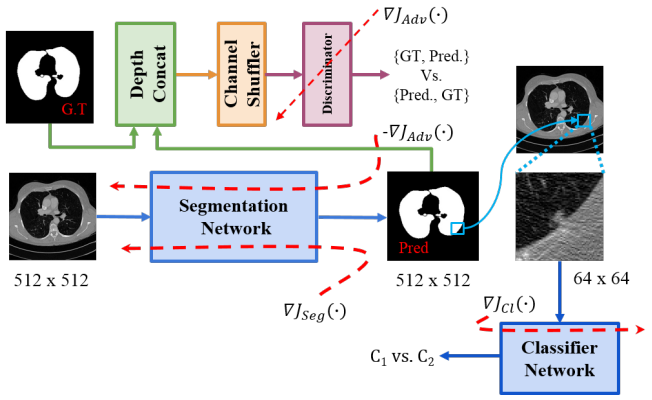


Fig. 1. Overview of the proposed method

Related works: Most of the existing methods propose to solve the problem of lung nodule detection through separate stages for lung and nodule segmentation. In one such method [3], lung segmentation has been performed using U-Net [4]. Recurrent residual convolutional neural network (RRCNN) [5] have also been used for the same. An improved version of U-Net [6], termed multi-scale prediction network (MPN) was proposed to solve lung area segmentation problems on thoracic CT scans. A fast and efficient 3D lung segmentation method based on V-net was proposed by [7]. In [8] the nodule detection task is performed in two stages. In the first stage, all possible candidate regions in CT slices are detected and in the later stage a 3D fully convolutional neural network (FCN) is used to detect nodules in the candidate regions with high certainty. Though this method presents high performance metrics, it also incurs high computational load in both stage for 3D processing.

Our approach: Considering the constraints and challenges associated with lung nodule detection, we propose a two stage framework as shown in Fig. 1 involving only 2D convolutional neural networks (CNNs). In the first stage we implement a fully convolutional network trained adversarially to segment the lung region and in the second stage a classifier network is trained to identify presence of nodules in image patches extracted from within the segmented lung region. The proposed method involves 2D processing with a

*This work supported through a research grant from Intel India Grand Challenge 2016 for Project MIRIAD

[1]Rakshith Sathish, Rachana Sathish and Debdoot Sheet are with the Department of Electrical Engineering, Indian Institute of Technology Kharagpur, India-721302 {rsatish, debdoot}@ee.iitkgp.ac.in, rachana.sathish@iitkgp.ac.in

[2]R. Sethuraman is with Intel Technology India Pvt. Ltd. Bangalore, India

compute complexity of 157.320×10^9 FLOPS (floating point operations) and 2.796×10^6 FLOPS per slice for first and second stage respectively.

II. Problem Statement

Consider a CT volume $\mathbf{V}$ consisting of N number of axial 2D slice $\mathbf{S}$. We model the problem of nodule detection in two stages. In *Stage 1*, each pixel of the slice $\mathbf{S_n}$ is classified into one of the two classes $\{lung, background\}$, to obtain a segmentation map. In *Stage 2* a two class classification problem is formulated where patches from the region identified as lungs in slice $\mathbf{S_n}$ is classified into a class $C_i \in \{C_1, C_2\}$. C_1 corresponds to presence of nodules and C_2 indicates its absence.

III. Method

The overall workflow is divided into two stages. In *Stage 1*, lung area is segmented followed by detection of nodules in *Stage 2*. Overview of the method is shown in Fig. 1.

Stage 1: Lung segmentation

A modified version of SUMNet [9] with batch-normalization is trained in *Stage 1* for segmentation of lungs in 2D slices of CT. The encoder of the network is similar to VGG16 [10] and is initialized with ImageNet pre-trained weights. The network has feature concatenation across convolutional blocks and propagation of indices across pooling layers from encoder to decoder. In addition to the structural segmentation loss, the network is trained using an additional adversarial loss similar to a generative adversarial network [11]. Fig. 3 shows the two steps of training involved in $Stage1$.

In each iteration of training, the discriminator is first trained to performs a Turing test to identify the ground truth (GT) and the segmentation map (Pred.) by presenting them together as the input to the network [12]. The concatenated input tensor of size $2 \times 512 \times 512$ is shuffled along the depth to randomize the order of the two channels as shown in Fig. 3(a). This ensures that the discriminator doesn't leverage the order of concatenation to differentiate between GT and Pred. The network is trained by minimizing the loss J_{Adv}, which is computed as the binary cross-entropy loss between its prediction ($\mathbf{o}_d$) and the true label ($\mathbf{t}_d$).

$$J_{Adv} = \mathbf{o}_d \log(\mathbf{t}_d) + (\mathbf{1} - \mathbf{o}_d) \log(\mathbf{1} - \mathbf{t}_d) \quad (1)$$

where $\mathbf{t}_d \in \{[1,0],[0,1]\}$ and depends on the order of shuffling. The architecture of discriminator is show in Fig. 2.

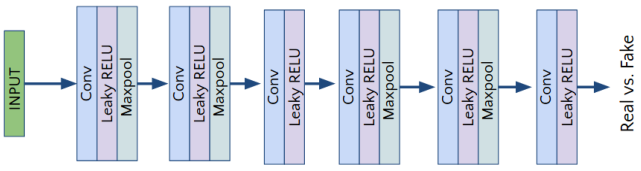
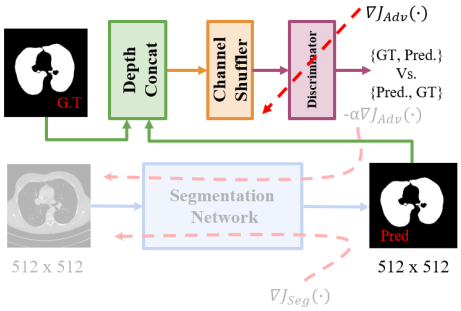


Fig. 2. Architecture of discriminator

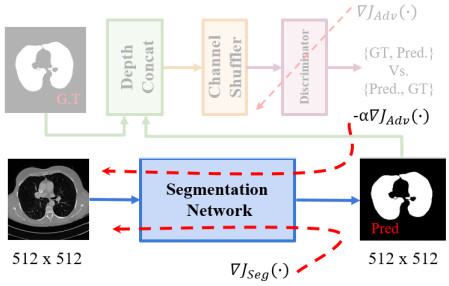
Next, the segmentation network is trained as shown in Fig. 3(b) using J_{Net} given as,

$$J_{Net} = J_{Seg} - \alpha J_{Adv} \quad (2)$$

where J_{Seg} is the cross entropy loss computed between the ground truth (GT) and the segmentation map ($Pred$). The hyper-parameter α, is chosen empirically to ensure similar magnitude of two losses.



(a) Training discriminator



(b) Training segmentation network

Fig. 3. Figure shows training of (a) discriminator and (b) segmentation network in *Stage 1*.

Stage 2: Detection of lung nodules

The nodules are significantly smaller in size in comparison with lungs. Therefore, patches of size 64×64 are extracted from the region segmented as lungs in each slice in *Stage 1* for further processing in *Stage 2*. A LeNet [13] based classifier is used to detect the presence of nodules in the patches as shown in Fig. 4. The third convolutional layer of the standard LeNet architecture is modified to have a kernel size of 5. An additional fully-connected layer having 256 neurons is introduced after the last sub-sampling layer. Also, the number of neurons in last layer is changed from 10 to 2. Thus, by evaluating patches within the lung region, the presence of nodules in each slice of the CT volume is determined

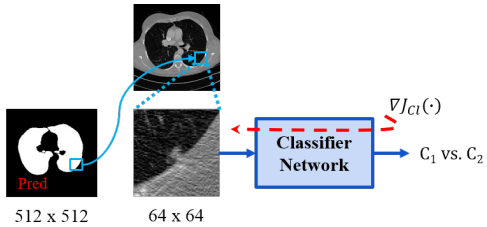


Fig. 4. Figure shows the overview of *Stage 2*. Class C_1 corresponds to presence of nodules and class C_2 corresponds to its absence.

IV. Experiments

Datasets: The proposed method is experimentally validated by performing 10-fold cross-validation on the LUNA16 challenge dataset[1]. The dataset consists of CT volumes from 880 subjects, provided as ten subsets for 10-fold cross-validation. In each fold of the experiment, eight subsets from the dataset was used for training and one each for validation and testing. The annotations provided includes binary masks for lung segmentation and, coordinates and spherical diameter of nodules present in each slice. LIDC-IDRI dataset[2] from which LUNA16 is derived has nodule annotations in the form of contours which preserves its actual shape. Therefore, we use annotations from LUNA dataset only in *Stage 1*. The annotations for the nodules from the LIDC dataset is used in *Stage 2* (nodule detection) to determine presence of nodules in image patches. The ground truth annotations were marked in a two-phase image annotation process performed by four experienced thoracic radiologists. Systematic sampling of slices from the CT volumes was performed to ensure equal distribution of slices with and without the presence of nodules.

Stage 1: Lung segmentation

Baselines: The following baselines were used for comparison of performance of *Stage 1*. **BL1**: UNet [4] trained using only J_{Seg}. **BL2**: R2UNet [5] trained using only J_{Seg}. **BL3**: SUMNet [9] trained using only J_{Seg}.

Training: The segmentation network and the discriminators were trained using Adam optimizer [14] for 35 epochs, with a learning rate of 10^{-4}. The loss scaling factor α in Eq. 2 was set as 0.001.

Stage 2 : Detection of lung nodules

The classification network for nodule detection was trained using $32,594$ patches of size 64×64 extracted from the lung region in the CT images, including the lung walls. Out of these patches, $16,440$ had partial or entire nodules accounting to $3,288$ in number. The model was trained for 50 epochs using Adam optimizer, with a learning rate of 10^{-4}.

V. Results and Discussion

Evaluation of lung segmentation

Quantitative evaluation: The performance of the proposed method and the baselines listed in Sec. IV for segmentation was evaluated using dice similarity coefficient (DSC),Area under the ROC Curve (AUC) and Hausdorff distance (HD).

$$DSC = \frac{2|Pred. \cap GT|}{|Pred.| + |GT|} \tag{3}$$

Tab. I presents the DSC, AUC Score and HD for fold 1 of the experimental setup. Due to the computational complexity of BL1 and BL2 which results in longer training duration, the performance evaluation was performed on only fold 1 of the dataset for these two methods. The mean and standard deviation of DSC across all ten folds of the experiments for BL3 and the proposed method is 0.980 ± 0.0018 and 0.984 ± 0.0007 respectively. The adversarial learning framework improves the performance consistently across all folds.

[1]https://luna16.grand-challenge.org/

[2]http://doi.org/10.7937/K9/TCIA.2015.LO9QL9SX

TABLE I

Quantitative metrics for lung segmentation (*Stage 1*).

Architecture	DSC	AUC	HD
BL1	0.979	0.9948	3.9424
BL2	0.983	0.9950	3.8754
BL3	0.980	0.9945	3.9596
Proposed method	0.983	0.9948	3.8989

Computational complexity: The number of trainable parameters and total floating point operations (TFLOPS) for the baselines and proposed method are shown in Tab. II. TFLOPS calculation was done for a sample input of size 512×512. It can be seen from Tab. II that the proposed method has lesser trainable parameters and involves significantly less number operations in comparison with the popularly used UNet (BL1) and R2UNet (BL2). Time taken to train the baselines and the corresponding model size is shown in Tab. III. All the networks were trained for 35 epochs on a GeForce GTX 1080 with 11GB RAM. Though the performance of the proposed method is comparable to that of BL2, it is computationally more efficient. The proposed framework can be trained $6\times$ faster with $1.6\times$ lesser memory requirement.

TABLE II

Total number of trainable parameters and FLOPS during inference.

Architecture	Parameters	TFLOPs
BL1	34,525,952 (34.526M)	261,901,254,656 (261.901G)
BL2	39,091,328 (39.091M)	612,076,355,584 (612.076G)
BL3	23,863,336 (23.863M)	153,538,789,376 (153.539G)
Proposed method	24,997,032 (24.997M)	153,538,789,376 (153.539G)

TABLE III

Comparison of computational complexity based on the total training time (35 epochs) and trained model size

Architecture	Training time	Model size
BL1	709m 37s	138.2 MB
BL2	2153m 11s	156.5 MB
BL3	326m 40s	95.5 MB
Proposed method	458m 17s	95.5 MB

Qualitative evaluation: The qualitative result of the segmentation of lungs for the proposed framework on a randomly chosen test image is shown in Fig. 5. The result of segmentation in the hilar region of lungs improves significantly with the proposed method.

Evaluation of nodule detection

Quantitative performance: The performance of the proposed method in detecting nodules is reported in terms of accuracy, sensitivity, and specificity of classification. Scores obtained are presented in Tab. IV. Explainability of ML



(a) Test image (b) Ground truth (c) Prediction of *Stage 1* (d) Result of image processing

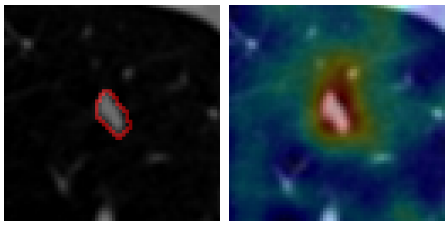
Fig. 5. Figure shows (a) a sample test image, (b) the corresponding ground truth (c) prediction of *Stage 1* and (d) result of classical image processing.

based methods is crucial in the field of medical image analysis. We have evaluated the trained classification network using RISE [15] to obtain a saliency map which assigns an importance score to each pixel of the input towards the model's prediction. Fig. 6 shows the saliency map for a randomly selected input patch which contains a nodule.

TABLE IV

PERFORMANCE OF THE CLASSIFICATION NETWORK

Metric	Score
Accuracy	98.00%
Sensitivity	0.9902
Specificity	0.9688



(a) Image patch (b) Saliency map

Fig. 6. Figure shows (a) sample image patch given as an input to the classifier network with the nodule marked in yellow (b) saliency map generated using RISE for positive prediction. In the colormap, red depicts high importance score and blue corresponds to a low score.

Computational performance: Classification network is computationally lighter in comparison with the segmentation network with a total of 50,162 (50.162K) trainable parameters and 2,796,448 (2.796M) floating point operations.

VI. CONCLUSION

In this paper, we propose a two stage framework for detection of lung nodules in CT slices. In the first stage, we segment the lung region using an adversarially trained CNN followed by detection of presence of lung nodules in image patches extracted from the lung region. We have achieved results comparable to the state-of-the-art architectures in terms of dice-coefficient score for segmentation and in terms of accuracy, specificity and sensitivity for the classification task, while being significantly less computationally expensive in terms of total number of parameters, total floating point operations, training time and model size. The additional loss from a discriminator used to train the network helps in improving the performance with very less increment in the computational complexity. Further, RISE based evaluation of explainability shows that the network attends to the relevant regions in an image while detecting the presence of a nodule.

REFERENCES

[1] WHO *et al.*, "World health organization cancer fact sheet," 2009.

[2] N. L. S. T. R. Team, "Reduced lung-cancer mortality with low-dose computed tomographic screening," *New England J. Med.*, vol. 365, no. 5, pp. 395–409, 2011.

[3] B. A. Skourt, A. El Hassani, and A. Majda, "Lung ct image segmentation using deep neural networks," *Proc. Comp. Sci.*, vol. 127, pp. 109–113, 2018.

[4] O. Ronneberger, P. Fischer, and T. Brox, "U-net: Convolutional networks for biomedical image segmentation," in *Int. Conf.n Med. Image Comput. Comp.-Assist. Interv.*, 2015, pp. 234–241.

[5] M. Z. Alom, M. Hasan, C. Yakopcic, T. M. Taha, and V. K. Asari, "Recurrent residual convolutional neural network based on u-net (r2u-net) for medical image segmentation," *arXiv preprint arXiv:1802.06955*, 2018.

[6] Y. Gu, Y. Lai, P. Xie, J. Wei, and Y. Lu, "Multi-scale prediction network for lung segmentation," in *Int. Symp. Biomed. Imag.*, 2019, pp. 438–442.

[7] M. Negahdar, D. Beymer, and T. Syeda-Mahmood, "Automated volumetric lung segmentation of thoracic ct images using fully convolutional neural network," in *Med. Imag.: Comp.-Aided Dia.*, vol. 10575, 2018, p. 105751J.

[8] L. Fu, J. Ma, Y. Chen, R. Larsson, and J. Zhao, "Automatic detection of lung nodules using 3d deep convolutional neural networks," *J. Shanghai Jiaotong Uni.*, vol. 24, no. 4, pp. 517–523, 2019.

[9] S. Nandamuri, D. China, P. Mitra, and D. Sheet, "Sumnet: Fully convolutional model for fast segmentation of anatomical structures in ultrasound volumes," in *Int. Symp. Biomed. Imag.*, 2019, pp. 1729–1732.

[10] K. Simonyan and A. Zisserman, "Very deep convolutional networks for large-scale image recognition," *Int. Conf. Learning. Repr.*, 2015.

[11] I. Goodfellow, J. Pouget-Abadie, M. Mirza, B. Xu, D. Warde-Farley, S. Ozair, A. Courville, and Y. Bengio, "Generative adversarial nets," in *Adv. Neu. Info. Proc. Sys.*, 2014, pp. 2672–2680.

[12] R. Sathish, R. Rajan, A. Vupputuri, N. Ghosh, and D. Sheet, "Adversarially trained convolutional neural networks for semantic segmentation of ischaemic stroke lesion using multisequence magnetic resonance imaging," in *Ann. Int. Conf. IEEE Engg. Med. Bio. Soc.*, 2019, pp. 1010–1013.

[13] Y. LeCun, L. Bottou, Y. Bengio, and P. Haffner, "Gradient-based learning applied to document recognition," *Proc. IEEE*, vol. 86, no. 11, pp. 2278–2324, 1998.

[14] D. P. Kingma and J. Ba, "Adam: A method for stochastic optimization," *Int. Conf. Learning Repr.*, 2015.

[15] V. Petsiuk, A. Das, and K. Saenko, "Rise: Randomized input sampling for explanation of black-box models," *Brit. Mach. Vis. Conf.*, 2018.